# Supplementary Materials

## "Thiol-ene" click synthesis of chiral covalent organic frameworks for gas chromatography

Jing-Xuan Guo,[a,b,c,d] Cheng Yang,[a,b,c] Xiu-Ping Yan[a,b,c,d] *

[a] State Key laboratory of Food Science and Technology, Jiangnan University, Wuxi 214122, China

[b] International Joint Laboratory on Food Safety, Jiangnan University, Wuxi 214122, China

[c] Institute of Analytical Food Safety, School of Food Science and Technology, Jiangnan University, Wuxi 214122, China

[d] Key Laboratory of Synthetic and Biological Colloids, Ministry of Education, Jiangnan University, Wuxi, 214122, China

*Corresponding author. E-mail address: xpyan@jiangnan.edu.cn (X.-P. Yan)

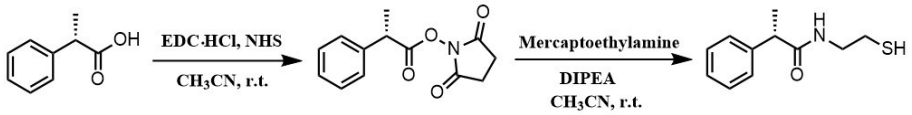


**Fig.S1** Synthesis route of (R)/(S)-*N*-(2-mercaptoethyl)-2-phenylpropanamide

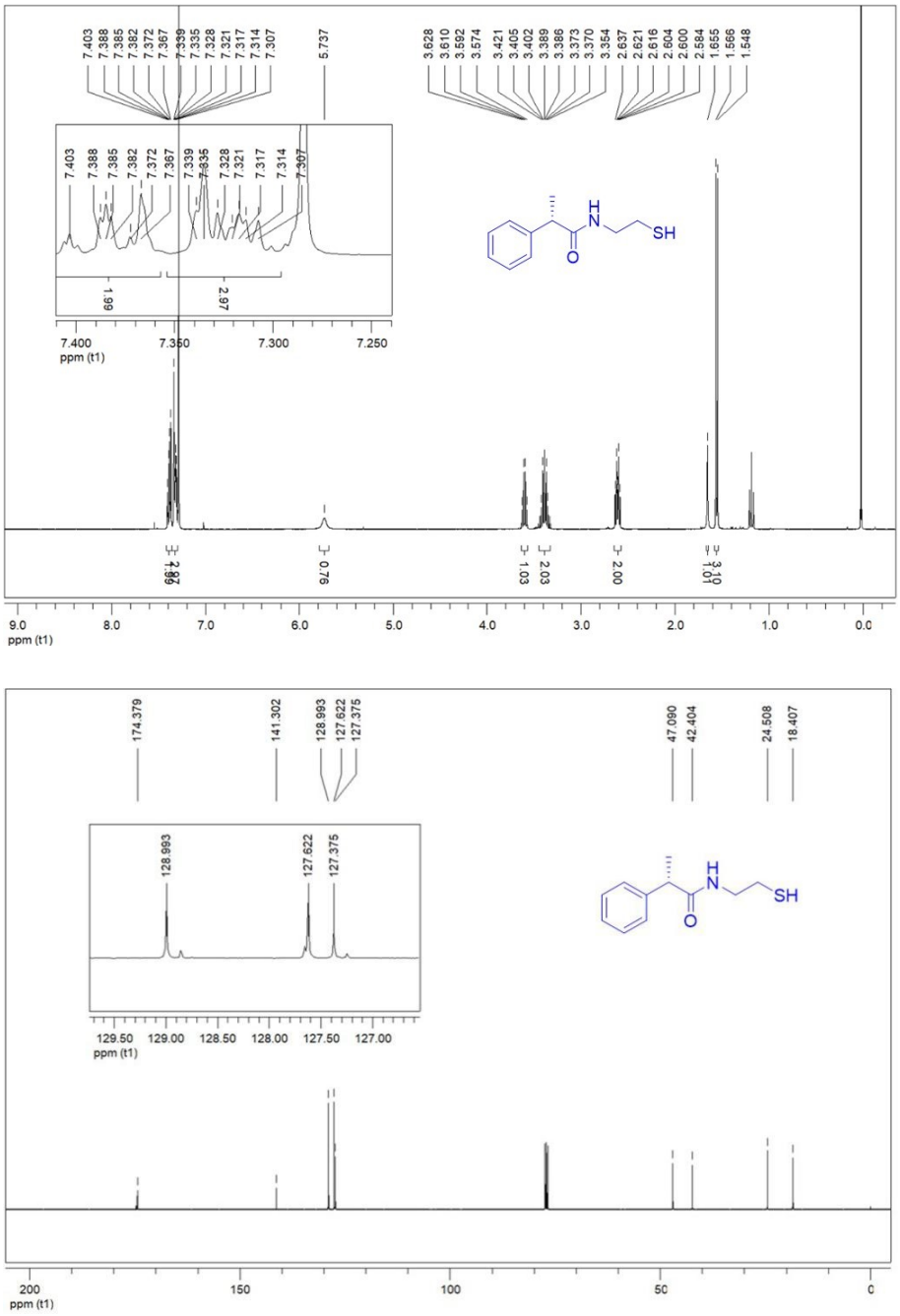


**Fig. S2** $^{1}H$ NMR and $^{13}C$ NMR spectrum of (S)-*N*-(2-mercaptoethyl)-2-phenylpropanamide in $CDCl_3$.

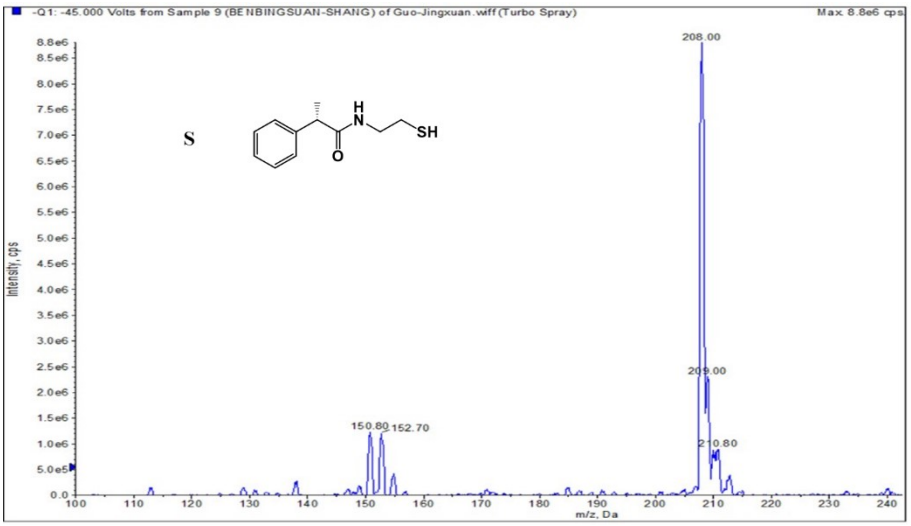


**Fig. S3** Mass spectrum of (S)-*N*-(2-mercaptoethyl)-2-phenylpropanamide.

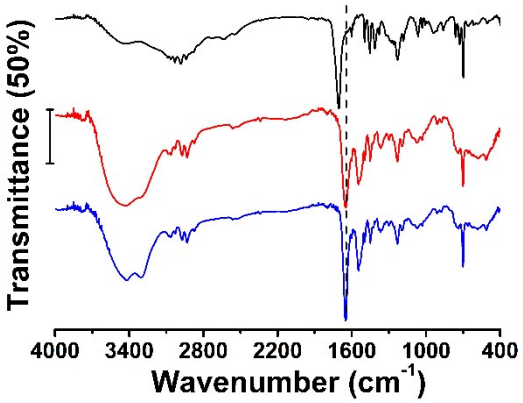


**Fig. S4** FT-IR spectra of (S)-2-phenylpropionicacid (black), (S)-*N*-(2-mercaptoethyl)-2-phenylpropanamide (red) and (R)-*N*-(2-mercaptoethyl)-2-phenylpropanamide (bule).

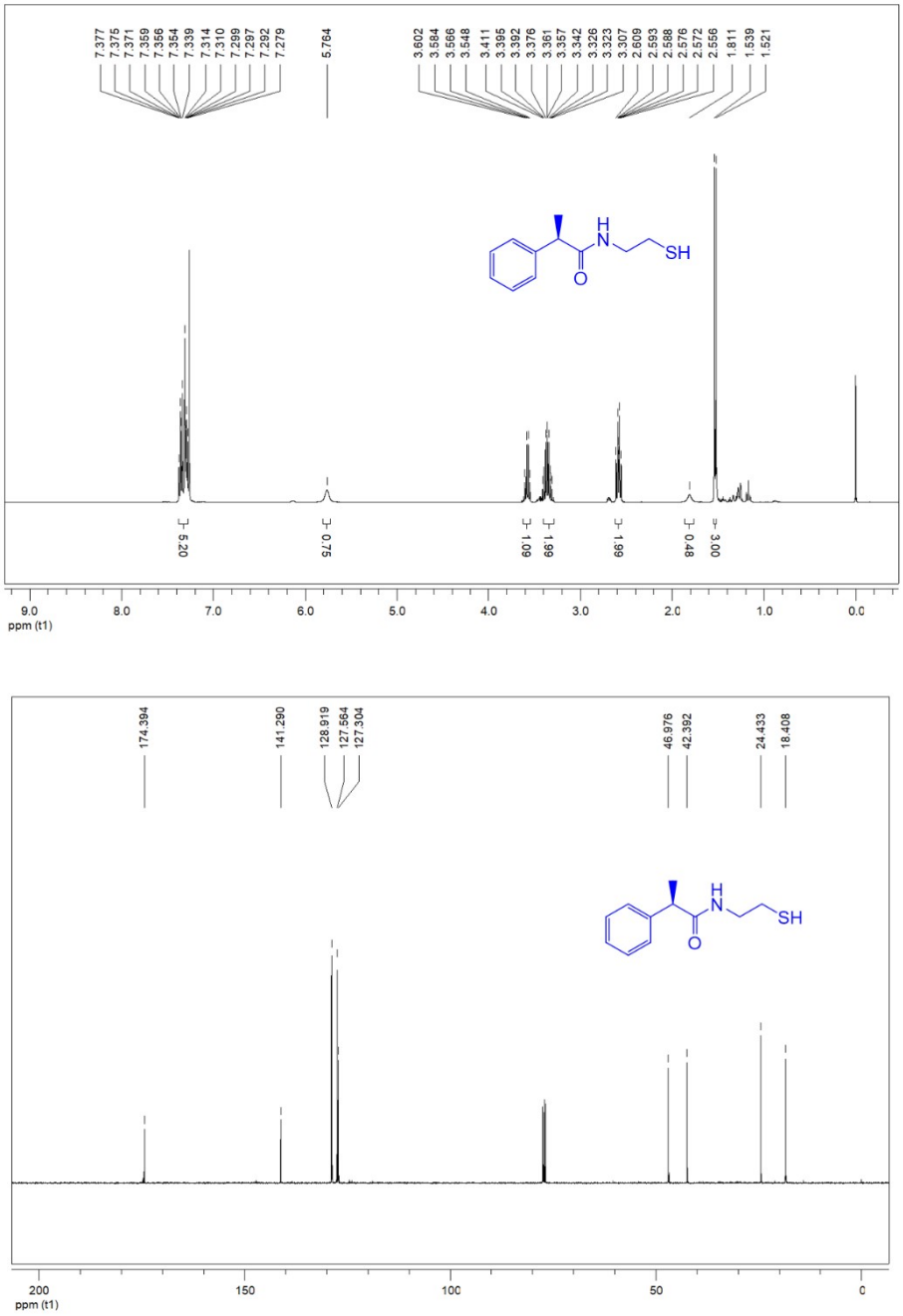


**Fig. S5** $^{1}H$ NMR and $^{13}C$ NMR spectrum of (R)-*N*-(2-mercaptoethyl)-2-phenylpropanamide in $CDCl_3$.

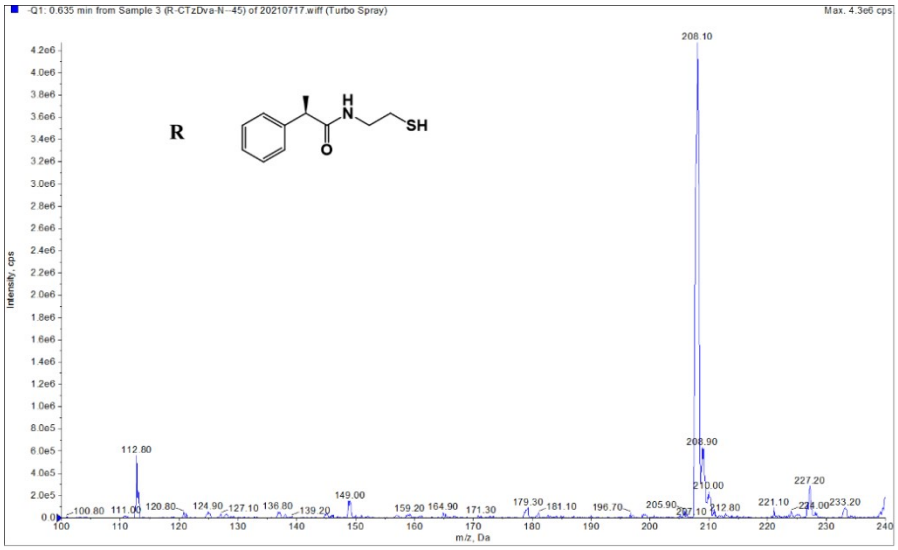


**Fig. S6** Mass spectrum of (R)-*N*-(2-mercaptoethyl)-2-phenylpropanamide.

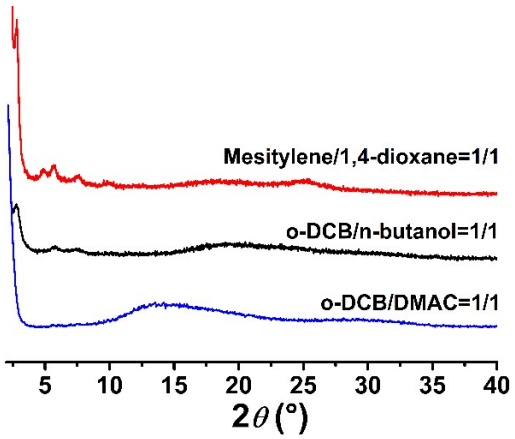


**Fig. S7** Effect of solvent type on the PXRD pattern of TzDva.

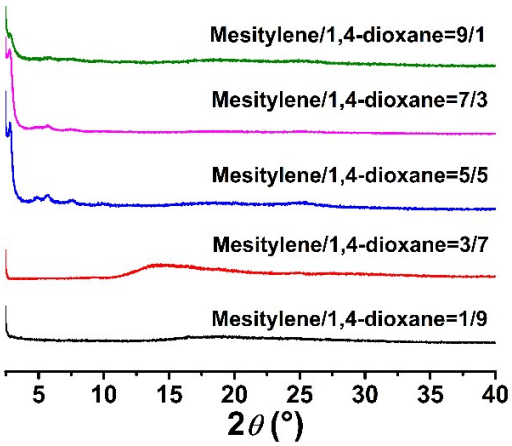


**Fig. S8** Effect of the volume ratio of mesitylene to 1,4-dioxane in binary solvent on the PXRD pattern of TzDva.

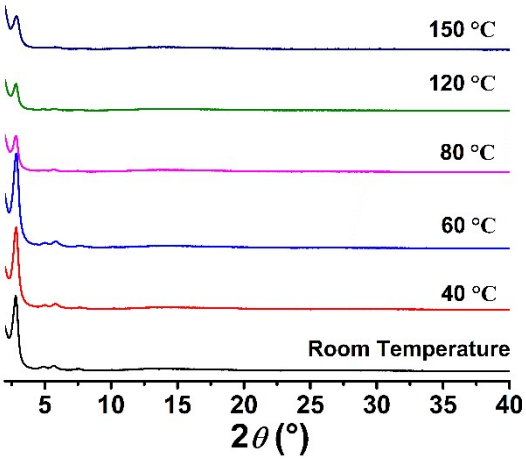


**Fig. S9** Effect of reaction temperature on the PXRD pattern of TzDva.

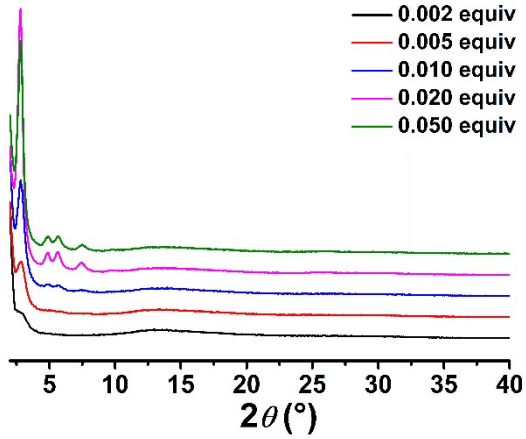


**Fig. S10** Effect of the amount of $Sc(OTf)_3$ on the PXRD patterns of TzDva.

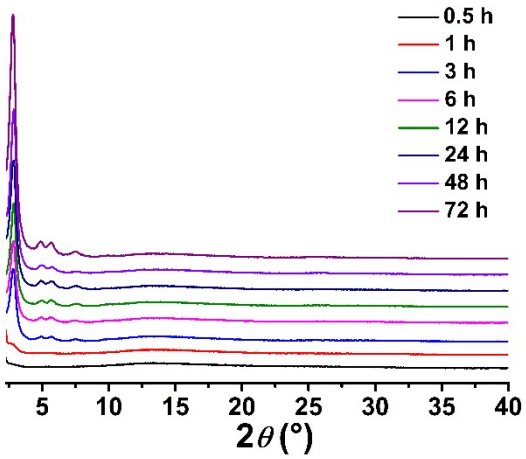


**Fig. S11** Effect of reaction time on the PXRD pattern of the TzDva.

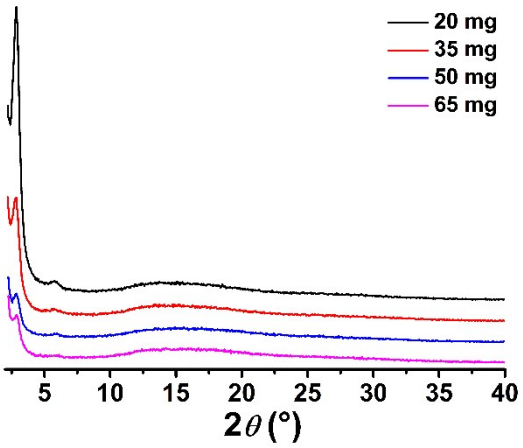


**Fig. S12** PXRD patterns of (S)-CTzDva prepared with different amounts of (S)-*N*-(2-mercaptoethyl)-2-phenylpropanamide.

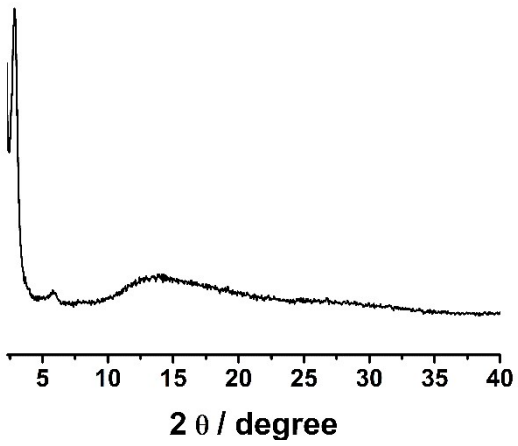


**Fig. S13** PXRD patterns of (R)-CTzDva.

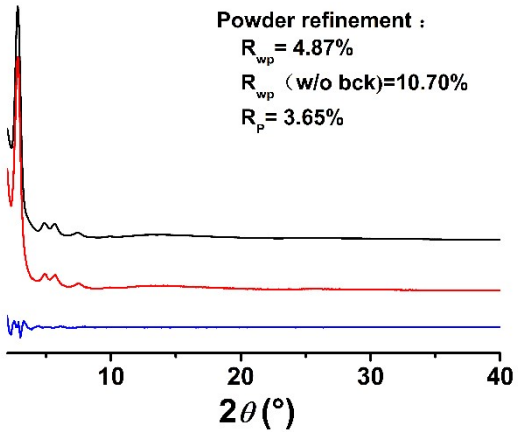


**Fig. S14** PXRD patterns of TzDva with experimental profiles in red, refined pattern in black and the difference between the experimental and refined PXRD patterns in blue.

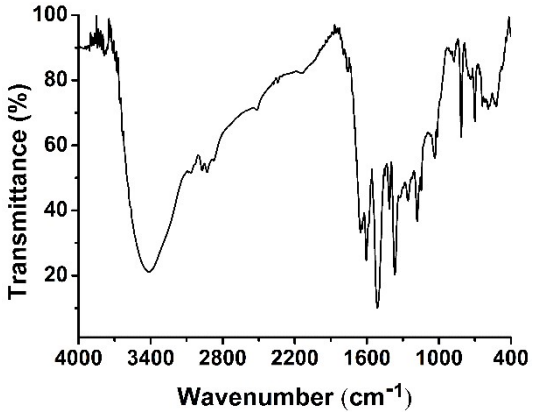


**Fig. S15** FT-IR spectra of (R)-CTzDva.

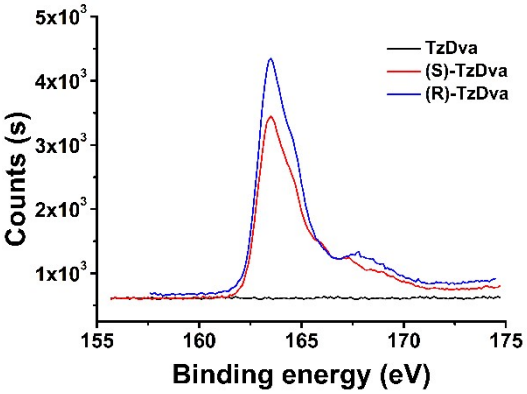


**Fig. S16** S 2p XPS spectra of TzDva and CTzDva.

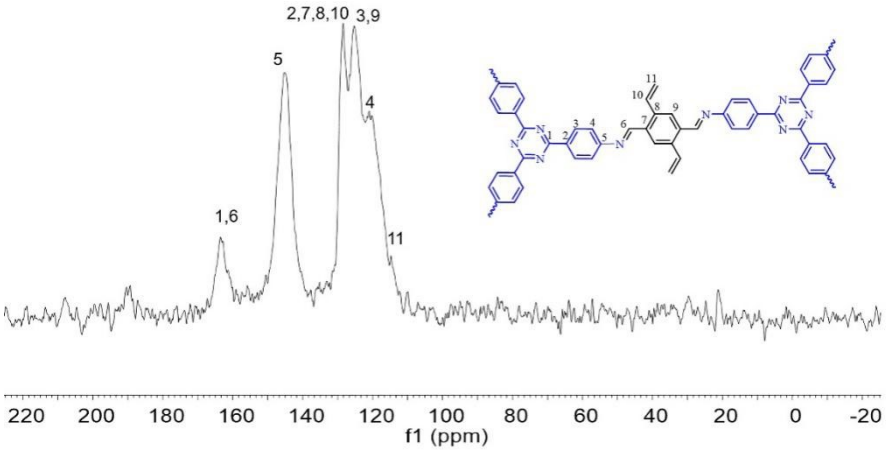


**Fig. S17** Solid $^{13}C$ NMR spectrum and peak contribution for TzDva.

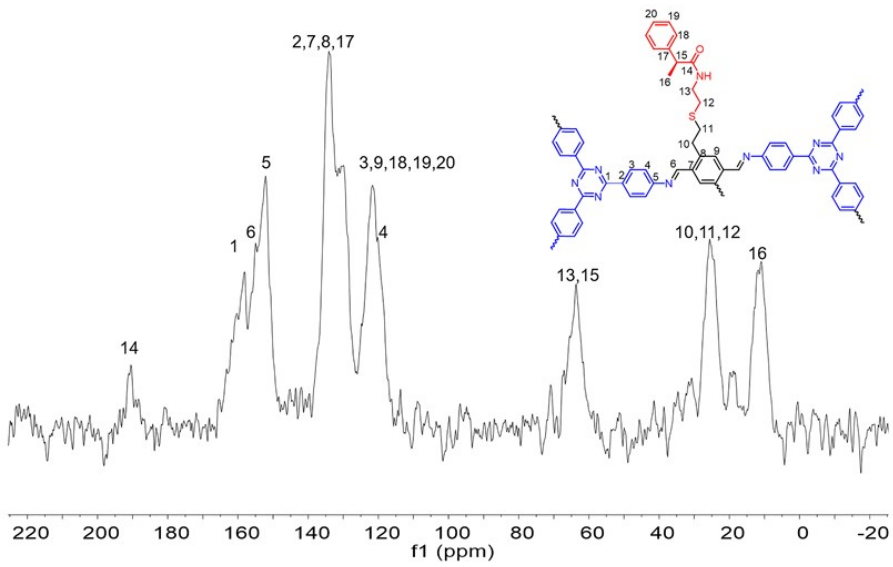


**Fig. S18** Solid $^{13}C$ NMR spectrum and peak contribution for CTzDva

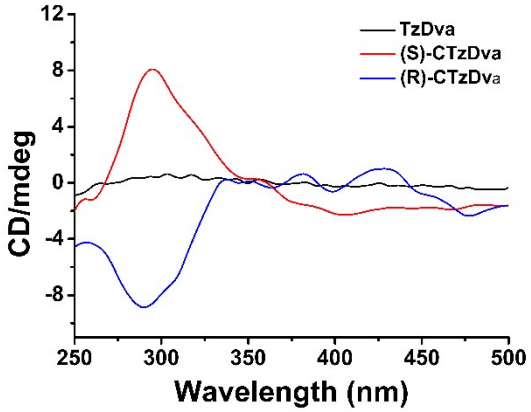


**Fig. S19** Circular dichroism spectra of TzDva and CTzDva.

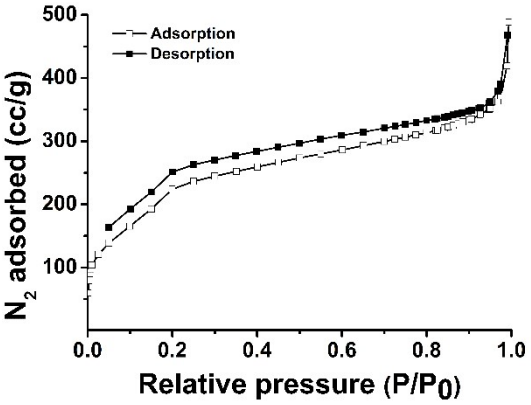


**Fig. S20** BET of (R)-CTzDva.

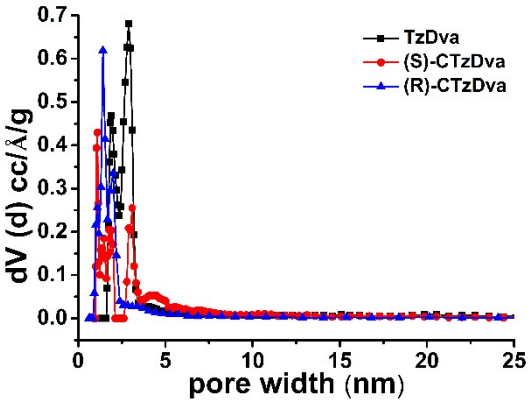


**Fig. S21** Pore size distribution of the as-prepared TzDva and CTzDva.

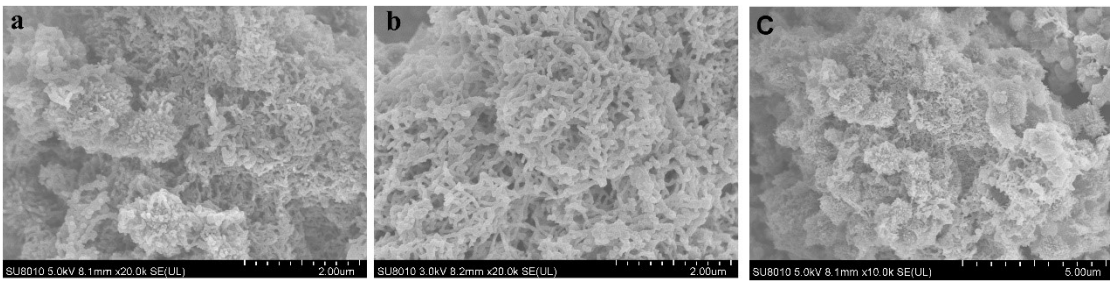


**Fig. S22** SEM images of TzDva (a), (S)-CTzDva (b) and (R)-CTzDva (c).

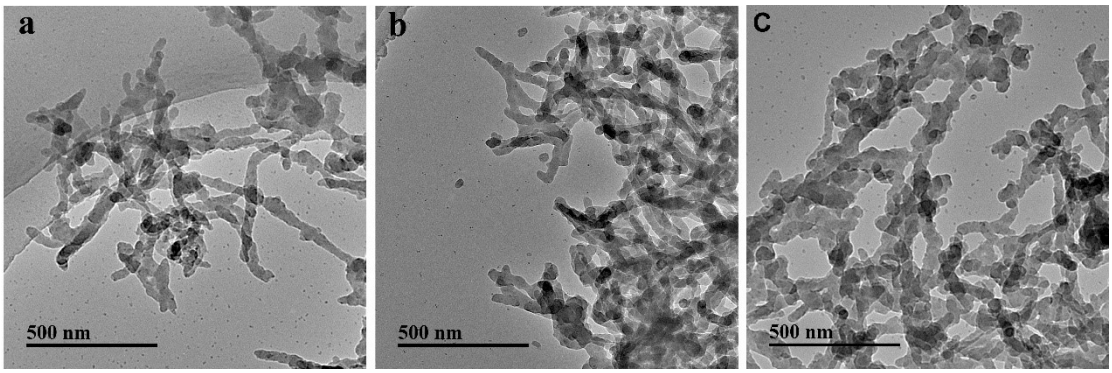


**Fi g. S23** TEM images of TzDva (a), (S)-CTzDva (b) and (R)-CTzDva (c).

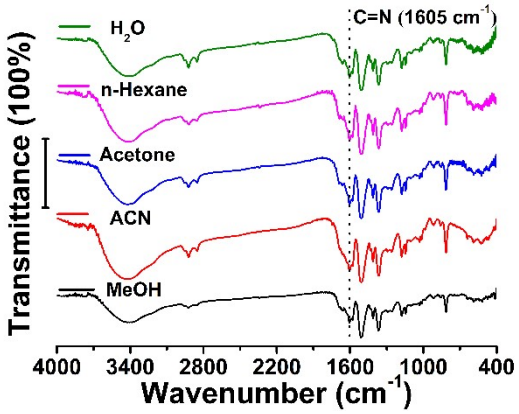


**Fig. S24** FT-IR patterns of TzDva after treatment with different solvents for 3 d.

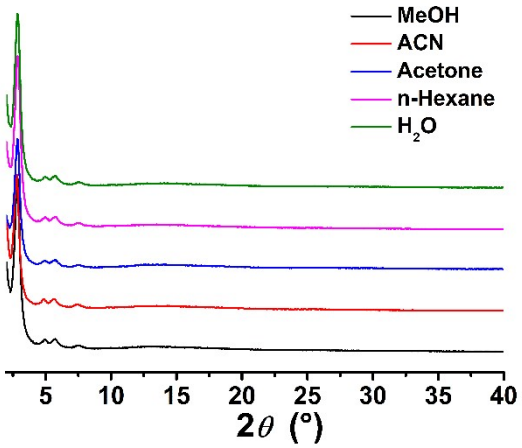


**Fig. S25** PXRD patterns of TzDva after treatment with different solvents for 3 d.

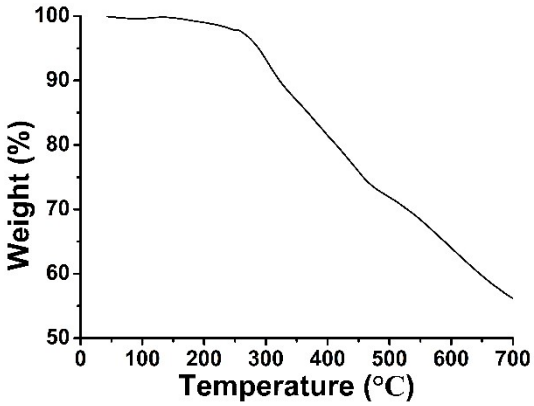


**Fig. S26** Thermogravimetric curves of (R)-CTzDva

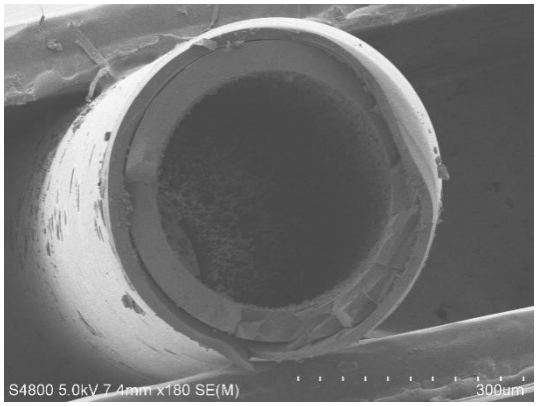


**Fig. S27** The SEM image of the inner wall of (R)-CTzDva coated capillary column.

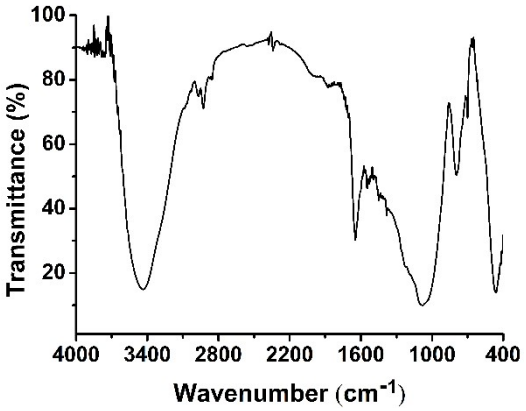


**Fig. S28** FT-IR spectra of (R)-CTzDva coated capillary column.

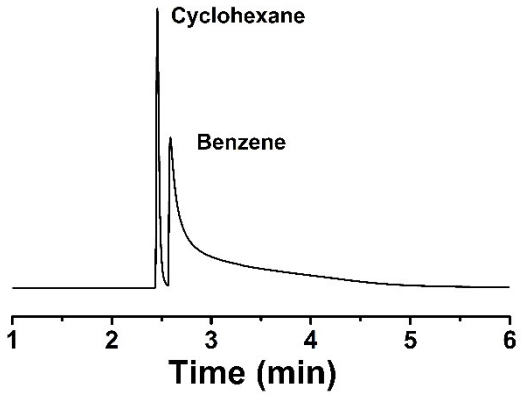


**Fig. S29** GC chromatograms on the CTzDva capillary column (30 m long × 0.32 mm i.d.) for the separation of benzene and cyclohexane at 60℃ under a $N_2$ flow rate is 1 mL $min^{-1}$

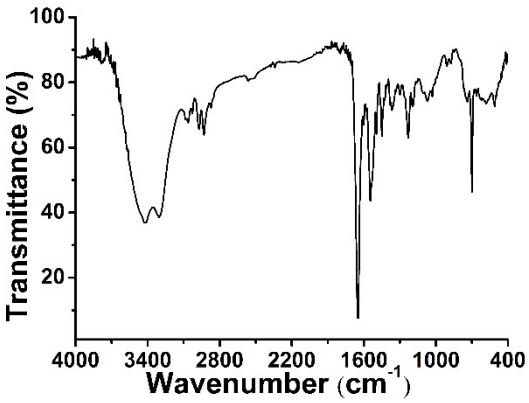


**Fig. S30** FT-IR spectra of (RS)-*N*-(2-mercaptoethyl)-2-phenylpropanamide.

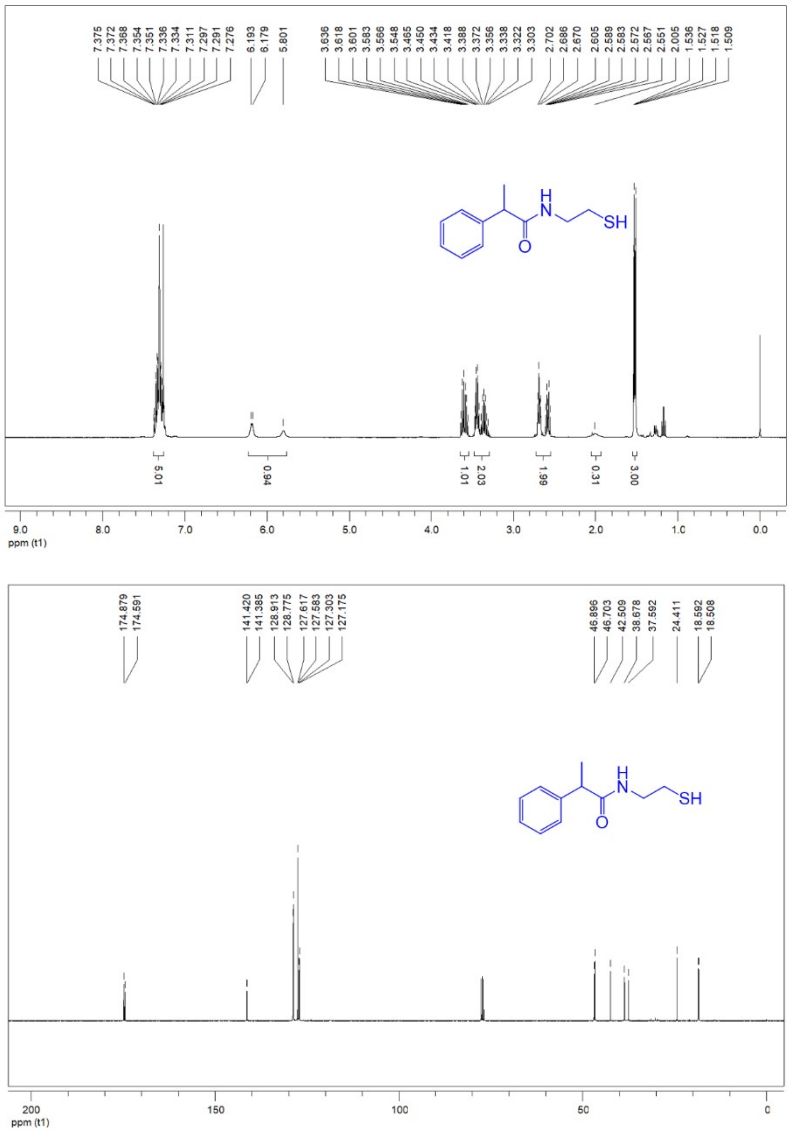


**Fig. S31** $^{1}H$ NMR and $^{13}C$ NMR spectrum of (RS)-*N*-(2-mercaptoethyl)-2-phenylpropanamide in $CDCl_3$.

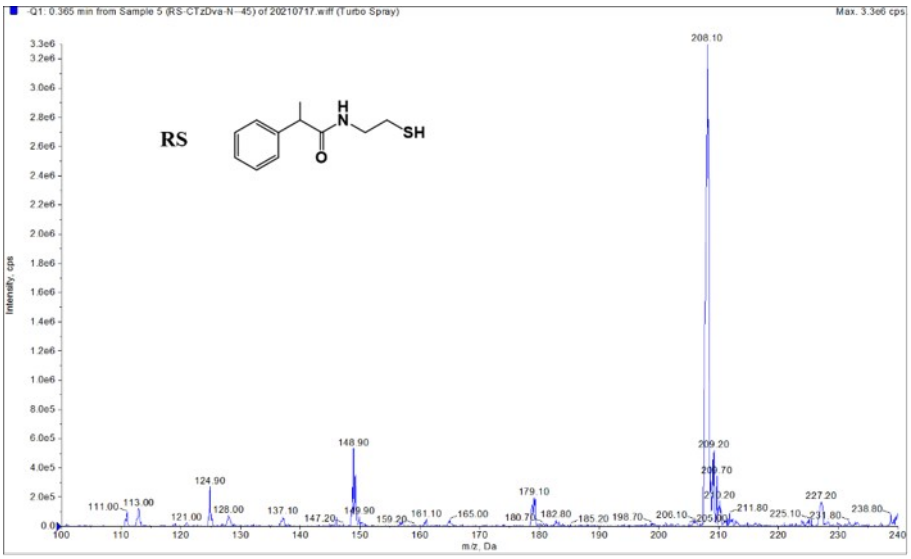


**Fig. S32** Mass spectrum of (RS)-*N*-(2-mercaptoethyl)-2-phenylpropanamide.

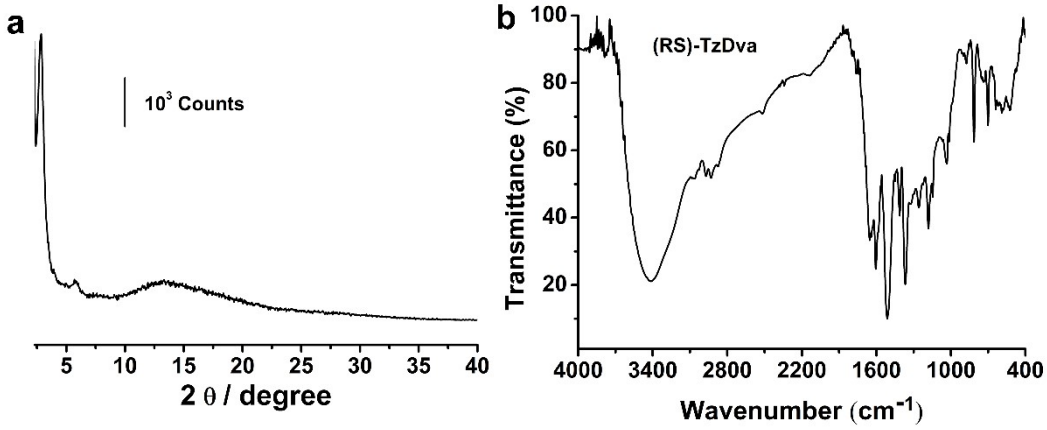


**Fig. S33** The PXRD pattern(a) and FT-IR spectra(b) of (RS)-TzDva.

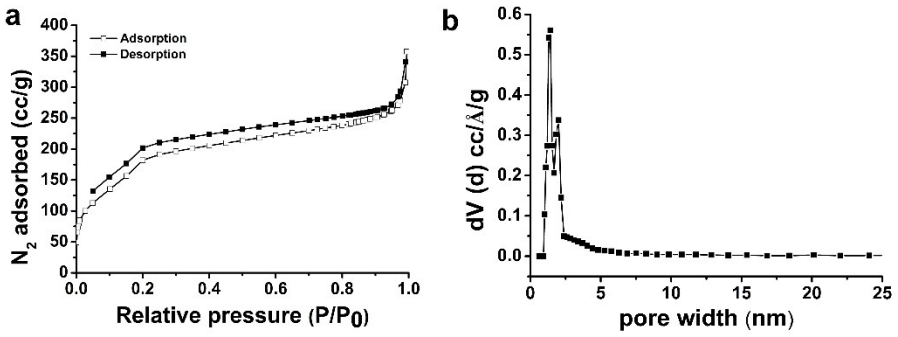


**Fig. S34** $N_2$ adsorption-desorption isotherms (a) and pore size distribution (b) of (RS)-TzDva.

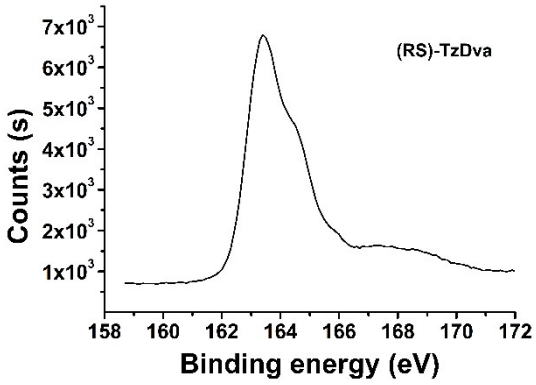


**Fig. S35** S 2p XPS spectra of (RS)-TzDva.

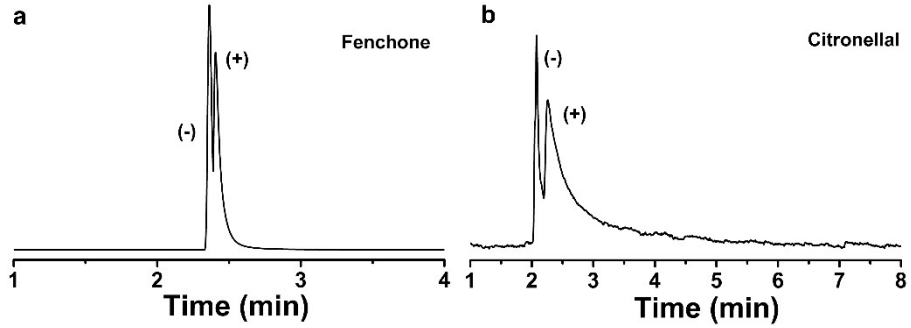


**Fig. S36** GC chromatograms on the (R)-CTzDva bonded capillary column (30 m long, 0.32 mm i.d.). (a) fenchone (150°C, 1 mL $min^{-1}$). (b) citronellal (160°C, 1 mL $min^{-1}$).

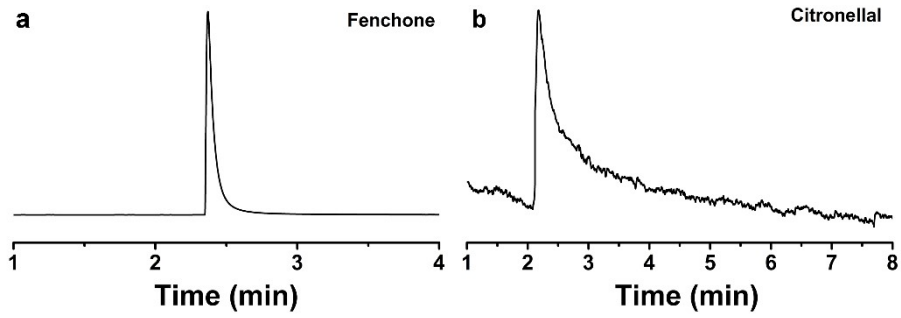


**Fig. S37** GC chromatograms on the (RS)-TzDva bonded capillary column (30 m long, 0.32 mm i.d.). (a) fenchone (150°C, 1 mL $min^{-1}$). (b) citronellal (160°C, 1 mL $min^{-1}$).

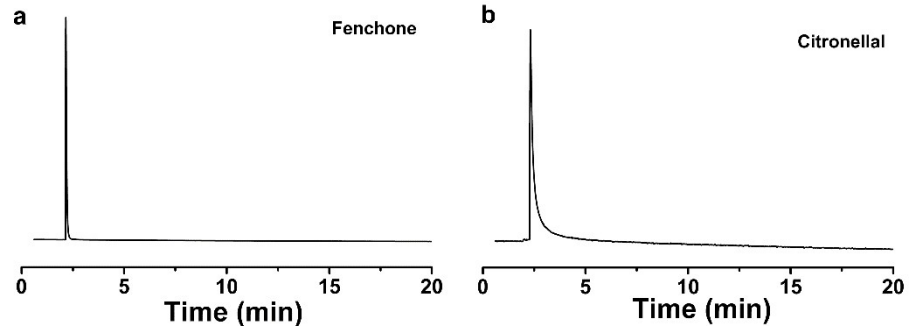


**Fig. S38** GC chromatograms on the (S)-*N*-(2-mercaptoethyl)-2-phenylpropionamide bonded capillary column (30 m long, 0.32 mm i.d.). (a) fenchone (150°C, 1 mL $min^{-1}$). (b) citronellal (160°C, 1 mL $min^{-1}$).

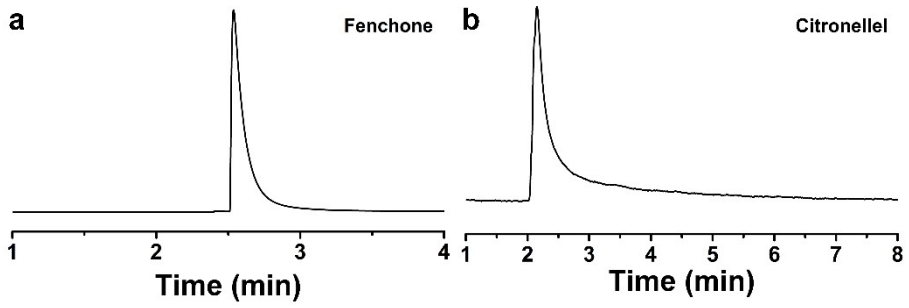


**Fig. S39** GC chromatograms on the TzDva coated capillary column (30 m long, 0.32 mm i.d.). (a) fenchone (150°C, 1 mL $min^{-1}$). (b) citronellal (160°C, 1 mL $min^{-1}$).

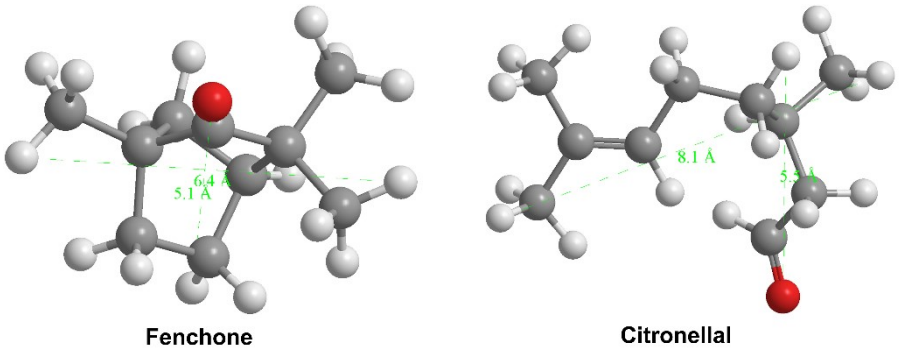


**Fig. S40** Structure and molecular dimension of the racemates (calculated with ChemBio3D Ultra).

**Table S1** Effect of reaction time on the yield of TzDva

| Reaction time | 0.5 h | 1 h | 3 h | 6 h | 12 h | 24 h | 48 h | 72 h |
|---|---|---|---|---|---|---|---|---|
| yield | 31.3% | 61.8% | 72.3% | 75.6% | 83.4% | 95.5% | 96.3% | 96.5% |

**Table S2** Elemental analysis of CTzDva prepared with different amounts of (S)-*N*-(2-mercaptoethyl)-2-phenylpropanamide.

| | C | N | S |
|---|---|---|---|
| 20 mg | 62.37% | 10.19% | 3.05% |
| 35 mg | 61.52% | 9.73% | 4.00% |
| 50 mg | 62.09% | 9.61% | 4.72% |
| 65 mg | 62.79% | 9.66% | 4.89% |

**Table S3** Fractional main atomic coordinates for the unit cell of TzDva after pawley refinement

TzDva: Space group symmetry P6/m, a= b = 36.1922 Å, c = 3.4399 Å, $\alpha = \beta = 90°$ and $\gamma = 120°$

| Atom | x | y | z |
|---|---|---|---|
| H1 | 0.33417 | 0.75454 | 0.97746 |
| N2 | 0.43227 | 0.88732 | 0.59212 |
| C3 | 0.43359 | 0.94979 | 0.96139 |
| C4 | 0.51649 | 0.98466 | 0.22836 |
| C5 | 0.48236 | 0.95787 | 0.45190 |
| C6 | 0.46397 | 0.91348 | 0.39874 |
| C7 | 0.46656 | 0.97443 | 0.73169 |
| C8 | 0.41389 | 0.84241 | 0.53821 |
| C9 | 0.38022 | 0.81806 | 0.79269 |
| C10 | 0.36236 | 0.77525 | 0.76260 |
| C11 | 0.41110 | 0.78267 | 0.25918 |
| C12 | 0.42968 | 0.82438 | 0.27748 |
| C13 | 0.37676 | 0.75696 | 0.49421 |
| C14 | 0.37676 | 0.75696 | 0.49421 |
| N15 | 0.31141 | 0.68544 | 0.47705 |
| H16 | 0.36914 | 0.83441 | 1.01101 |
| C17 | 0.41745 | 0.91180 | 0.91087 |
| H18 | 0.47885 | 0.90167 | 0.17161 |
| H19 | 0.53018 | 0.97114 | 0.00594 |
| H20 | 0.42730 | 0.76853 | 0.05498 |
| H21 | 0.45383 | 0.84575 | 0.07689 |
| H22 | 0.54273 | 0.57791 | 1.18993 |
| H23 | 0.46386 | 0.56527 | 0.72932 |
| H24 | 0.50419 | 0.61506 | 1.04472 |

**Table S4** Comparison of CTzDva coated capillary columns and other chiral columns for chiral separation

| Column | (+/-)-Fenchone | | (+/-)-Citronellal | |
|---|---|---|---|---|
| | R | Retention time (min) | R | Retention time (min) |
| CTzDva | 1.38 | 2.35 | 1.06 | 2.07 |
| CP-Chirasil Dex CB | 1.55 | 26.77 | 0 | 4.89 |
| Cyclosil-B | 0 | 6.34 | 0 | 8.21 |
| MIL-101-S-2-Ppa[1] | 1.20 | 2.15 | - | - |
| MIL-101-R-Epo[1] | 1.67 | 1.96 | - | - |

- Not available

**Table S5** Precision of retention time of chiral analytes on CTzDva coated capillary columns

| Enantiomers | RSD (%) | |
|---|---|---|
| | Run-to-run（n=7） | Day-to-day（n=5） |
| (-)-Fenchone | 0.7 | 2.2 |
| (+)-Fenchone | 0.3 | 0.5 |
| (-)-Citronellal | 0.5 | 2.4 |
| (+)-Citronellal | 0.2 | 1.9 |

## Reference

1. W. T. Kou, C. X. Yang, and X. P. Yan, 2019, J. Mater. Chem. A, 2018, 6, 17861-17866.